Published in Physical Review B 53, issue 15, 10209-10216, 1996
which should be used for any reference to this work

Final-state scattering in angle-resolved ultraviolet photoemission from copper

Jürg Osterwalder and Thomas Greber
Physik-Institut, Universität Zürich-Irchel, Winterthurerstrasse 190, CH-8057 Zürich, Switzerland

Philipp Aebi, Roman Fasel, and Louis Schlapbach
Institut de Physique, Université de Fribourg, CH-1700 Fribourg, Switzerland

The problem of direct transition intensities in angle-resolved UV photoelectron spectroscopy is addressed. We demonstrate that the angular distribution of intensities integrated over the full $3d$ band of copper is dominated by final-state scattering effects much like those observed in the diffraction of core level photoelectrons. These UV photoelectron diffraction effects are very sensitive to the angular momentum character of the valence orbitals that form the band states, and to the atomic structure of the surface layers. Specifically, we have performed measurements on Cu(111) and Cu(001) surfaces where we find excellent agreement of experimental angular distributions of integrated *d* band emission excited by He I and He II radiation and single-scattering cluster calculations, involving emission from *localized d* states, and including proper photon polarizations. At the same time the angle-resolved energy spectra show strong dispersion effects, reflecting the *delocalized* character of these band states. This duality may be a further indication for the localization of the valence hole upon photoemission.

I. INTRODUCTION

Angle-resolved ultraviolet photoelectron spectroscopy (ARUPS) has been, over the last two decades, an exceedingly successful technique for mapping electronic energy bands of solids[1,2] and surfaces.[3] Data interpretation is very direct and relies, to first approximation, on the conservation laws of energy and momentum in the photoemission process. In brief, the spectra show direct transition (DT) peaks at those photoelectron kinetic energies and momenta where **k**-vector conserving transitions between initial and final-state bands exist with energy separations equal to the photon energy. Accordingly, the measurable quantities are, for a given photon energy, energy positions and emission angles.

ARUPS spectra contain, however, additional information about the system under study: It is well recognized that the intensities of the direct transition peaks depend on the symmetry of the local orbitals that constitute the initial band states.[1,2] Experiments performed along mirror planes of single-crystal samples, and with photon polarization vectors normal to these planes, can easily discriminate between even or odd state symmetries with respect to these planes. Photoemission matrix elements either suppress or enhance states with respective symmetries. Apart from such qualitative matrix element arguments, it is considered very difficult to extract information from intensity variations of direct transition peaks.[4] While theoretical formalisms exist that include the effects of matrix elements and final-state scattering,[5–8] in practice most analyses of ARUPS measurements to date use free-electron final states. In very early work on TaS_2 (Ref. 9), the multiple-scattering character of the final state has been found important to explain details in the angular distribution of Ta *d* emission.[10] We investigate in this paper, experimentally and theoretically, the influence of final-state scattering on the intensities of direct transition peaks from the $3d$ band of copper. In contrast to the spectra measured from TaS_2 (Ref. 9), we observe strong dispersion effects in Cu, making this an excellent case for studying the interrelation between dispersion and intensities of direct transition peaks.

Our interpretation of photoemission intensities emphasizes the effects of photoelectron scattering and diffraction. This approach has been used very successfully over the last few years for describing angular distributions of core level photoemission intensities.[11] In this case, a spherical photoelectron wave emanating from the photoemitting atom is considered. This wave is scattered strongly by the core potentials of the neighboring atoms, and a highly anisotropic emission pattern evolves which carries information on the local atomic structure around the photoemitter. These phenomena can be conveniently modeled by scattering cluster calculations, and photoelectron diffraction can thus be used for determining surface atomic structure.[11]

II. THE IDEA

Our quantitative measurements of valence emission intensities in ARUPS are based on an acquisition procedure analogous to that used in photoelectron diffraction experiments: The photoelectron current within a suitable energy window is recorded sequentially while a single-crystal sample is rotated to sweep the photoelectron emission direction across a large part of the hemisphere above the surface.[12] The important point is that we have a constant flux of photons and a fixed orientation of the electron energy analyzer relative to the photon incidence direction. In Fig. 1 we illustrate the relationship between an arbitrarily defined energy window and the measured total intensity for the case of the fast-dispersing sp-band transitions from Cu(111). Note that the background in these spectra is rather low and we therefore do not take any measures to subtract it.

If the energy window is narrower than the bandwidth, such as shown in Fig. 1, there are obviously two different

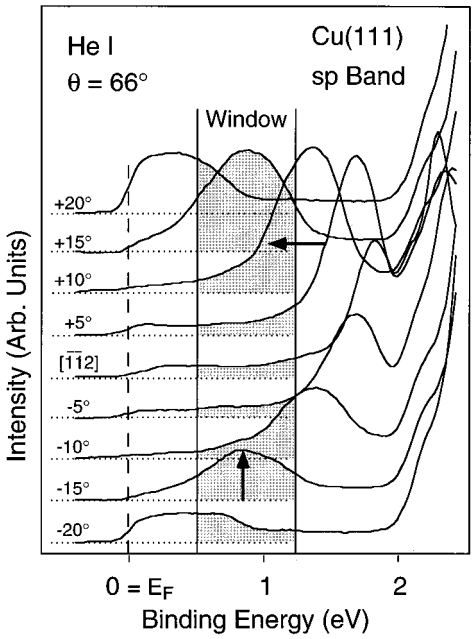

FIG. 1. He I (21.2 eV) excited photoelectron spectra from Cu(111) at a polar angle of 66° for various azimuthal angles relative to the [1 12] azimuth. Shaded areas represent the measured intensities inside an arbitrary energy window within the *sp* band energy range. The horizontal arrow indicates how these intensities vary due to the direct transition peak moving through the energy window, while the vertical arrow symbolizes variations of direct transition intensities (see text).

processes that modulate the measured intensity: At emission directions where a direct transition disperses through the window, the intensity takes a high value while it is low at all other directions. If we compare two spectra where the transition is centered on the window, we find still different intensities: The DT intensity is modulated by transition matrix elements. For arbitrarily chosen windows smaller than the overall bandwidth these two processes mix, and the resulting intensity modulations are difficult to interpret. However, there are two important limiting cases: If a very narrow window is selected, we can use the measured intensities for a very accurate **k**-space mapping of states with a binding energy given by the position of the chosen energy window. Of particular interest are measurements with a narrow window located at the Fermi energy which permits a direct mapping of Fermi surfaces for two- and three-dimensional systems.[13–17] The other limiting case, which is the one we deal with in this work, is where the energy window is matched to the entire bandwidth. In this case the DT peak never disperses out of the measurement window, and the intensities thus reflect directly the processes of the second type, i.e., we measure matrix elements. This experiment obviously cannot be carried out with the *sp* band of copper, because it traverses the Fermi energy. We have therefore concentrated on the more localized 3*d* band, which is completely occupied and very well characterized in terms of band dispersion and upper and lower band edges.[2]

III. EXPERIMENTAL

The experiments were carried out in a Vacuum Generators ESCALAB Mark II photoelectron spectrometer at a base

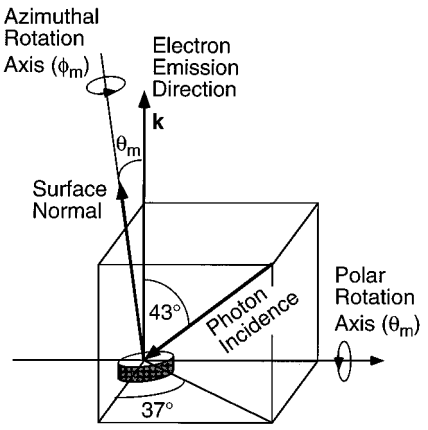

FIG. 2. Experimental geometry used for these measurements. Electron emission and photon incidence directions are fixed with respect to each other while the single-crystal sample is rotated about polar and azimuthal axes. Note that the photon incidence vector is not within the plane swept by the sample surface normal.

pressure of 2×10^{-11} mbar. The Cu(111) and Cu(001) single-crystal samples were prepared using standard techniques in order to present atomically clean and well-ordered surfaces and then *in situ* mounted on a computer-controlled two-axis goniometer. The spectrometer, consisting of a magnifying (3:1) lens, a 150-mm hemispherical-sector analyzer and a three channeltron detector unit, was set to accept photoelectrons within a narrow acceptance cone of the order of 3° full opening angle by adjusting an iris aperture in front of the lens. The unmonochromatized He discharge lamp was mounted at a fixed angle relative to the lens axis and the sample tilt axis (Fig. 2). A stable operation of the lamp over the typical measuring times of the order of 2 to 3 h was crucial for this experiment and was achieved by maintaining a constant pressure behind the He inlet leak valve.

Complete angular distributions of photoelectrons were measured by sweeping the emission direction, i.e., the lens-analyzer entrance direction, in consecutive azimuthal circles over almost 2π solid angle relative to the crystal surface by computer-controlled crystal rotation.[12] At each of typically 4000 angular settings the spectral range of interest is measured and the intensity integrated over the entire 3*d* bandwidth ranging from 2.0 to 5.6 eV in binding energy. For presentation purposes the angular mesh is stereographically projected and the intensities are plotted in a linear gray scale.

Due to the combination of a relatively small UV beam diameter and photoelectron analysis spot, strong and purely instrumental intensity variations occurred with polar emission angle. In order to circumvent this problem, overall polar intensity variations have been removed by normalizing the data on each azimuthal scan. This same procedure has been carried out for calculated intensity patterns to give a meaningful comparison.

Before measuring the UV excited intensity patterns, the crystal axes were determined to an accuracy of $\sim$0.2° by means of x-ray photoelectron diffraction using the same setup and an Mg Kα x-ray source.[18]

IV. THEORETICAL APPROACH

The scattering theory describing the emission of core-level photoelectrons from well-ordered crystal surfaces is

well established.[11] Due to the short *inelastic* mean free paths of excited electrons in solids, ranging from only a few Å to a few tens of Å depending on the kinetic energy, the *elastic* scattering is conveniently treated in a cluster approximation, with clusters representing the local atomic environment of near-surface photoemitters. The important point is here that, for well-localized core levels, a photoelectron wave is considered to be emanating from a single, well-identified atom within this cluster. This wave is then scattered coherently by all atoms to produce a diffraction pattern characteristic for this particular emitter site. All atoms within the surface region act as photoemitters and their individual diffraction patterns add up incoherently. Diffraction patterns have to be calculated for all inequivalent emitter sites. For Cu(111) and Cu(001) surfaces this means that one emitter per atomic layer needs to be considered. The results presented in the next section are for clusters with four layers containing a total of about 150 Cu atoms. We find this cluster size to be essentially converged.

The calculations have been carried out within the single-scattering cluster (SSC) approximation[11] which is known to be efficient and to describe photoelectron diffraction data rather accurately in many cases. The individual electron-atom scattering processes include effects due to the spherical-wave nature of emitted and scattered photoelectron waves: For a given initial state of angular momentum l and for a given photon polarization state a highly anisotropic wave is emitted. The associated curvature effects at the scatterer site are known to be important at low electron energies.[19] For calculating effective scattering matrices we use the very efficient and accurate formalism of Rehr and Albers[20] which has been implemented for use in a single-scattering cluster code by Friedman and Fadley.[21]

The experiments have been performed using unpolarized He I and He II radiation. This can be modeled by incoherent superposition of two calculations using orthogonal photon polarizations within a plane normal to the photon incidence direction. For each one of these polarization vectors emission from a Cu $3d$ state produces waves of p and f symmetry by applying dipole selection rules. For a filled shell all magnetic quantum numbers $m=0, \pm1, \pm2$ have to be considered with equal weight, and p and f channels of equal m interfere with each other, with radial matrix elements and phase shifts taken from atomic calculations.[22] Emission from s and p initial states are calculated accordingly.

Partial wave phase shifts for calculating spherical-wave scattering amplitudes have been obtained within a muffin-tin approximation analogous to those used for low-energy electron diffraction.[23] An inner potential V_0 of 13.5 eV (Ref. 23) was used in order to consider wave refraction effects at the surface potential step, as well as a work function Φ of 4.9 eV. Final-state scattering was then calculated for a kinetic energy corresponding to photoexcitation from the mean $3d$ band energy: i.e., $E_B^{3d}=[(2.0+5.6)/2]\text{eV}=3.8$ eV. For a given photon energy the kinetic energy inside the crystal results in

$$E_{\text{kin}}^{\text{solid}}=h\nu-E_B^{3d}-\Phi+V_0, \tag{1}$$

and we obtain values of 26.0 eV (He I, $h\nu=21.2$ eV) and 45.6 eV (He II, $h\nu=40.8$ eV). At such low energies refraction effects are very important. We find only a moderate energy dependence of the intensity patterns for variations of the kinetic energy within the $3d$ bandwidth.

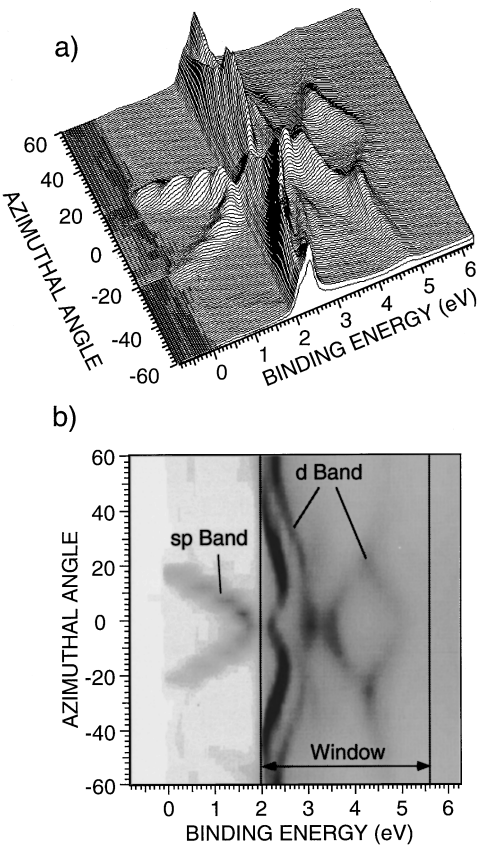

FIG. 3. Series of electron spectra from Cu(111), excited by He I radiation. Spectra were taken every 5° of azimuthal emission angle, at a polar angle of 66° off normal. In (a) the spectra are represented as a relief plot, with intensities *not* normalized with respect to each other. Sinusoidal oscillations on the parabolic sp band (0–2 eV) are an artifact due to the two-dimensional interpolation of the data to produce this graph. The origin of the azimuthal angle scale is along the $[\bar{1}\,12]$ azimuth. In (b) the same data are given in a linear gray scale presentation which permits a better definition of the energy window used for obtaining the data given in Figs. 4–7.

V. RESULTS AND DISCUSSION

In Fig. 3 a series of He I excited angle-resolved valence band spectra from Cu(111) are presented, measured at 5° intervals over one symmetry-equivalent stretch of 120° in azimuthal angles, at an arbitrary polar angle of 66° off normal. In order to give the connection between the actual spectra and the integration procedure used in the following, we chose to give a representation both as a relief plot [Fig. 3(a)], emphasizing the highly dispersive character of the energy spectra in both the sp and $3d$ spectral ranges, and as a grey scale plot [Fig. 3(b)] showing the energy window selected for the intensity scans (Figs. 4 to 8). The parabolic sp band can be seen clearly between the Fermi energy and 2 eV binding energy, where the top of the $3d$ band is marked clearly with a steplike increase in background intensity and strong, slighly less dispersing emission features. Still, direct transitions are found moving over the entire d bandwidth.

In Figs. 4 to 7 we give the results of our measurements

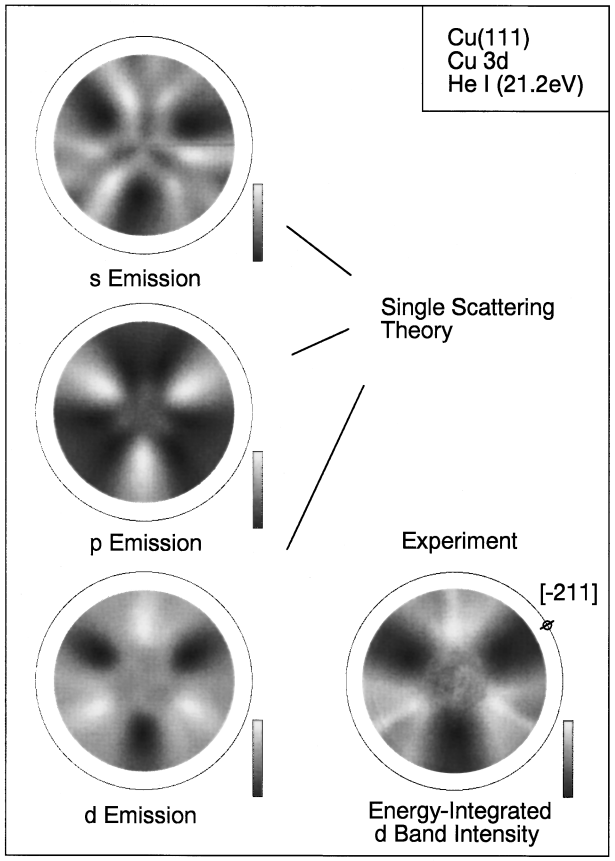

FIG. 4. Complete angular distributions of Cu 3*d* electrons from Cu(111), measured with He I radiation. The data have been stereographically projected and intensities are given in a linear gray scale after being normalized to equal average value along each azimuthal circle (see text). The center of each plot represents normal emission, while the outer circle indicates emission directions parallel to the surface. The experimental curve (bottom right) has been obtained by measuring the total intensity within the energy window indicated in Fig. 3(b) for 3600 angular settings spread uniformly over the measured solid angle reaching out to 78° in polar angle. Single scattering cluster calculations (left row) for emission from localized *s*, *p*, or *d* emitters are shown for comparison.

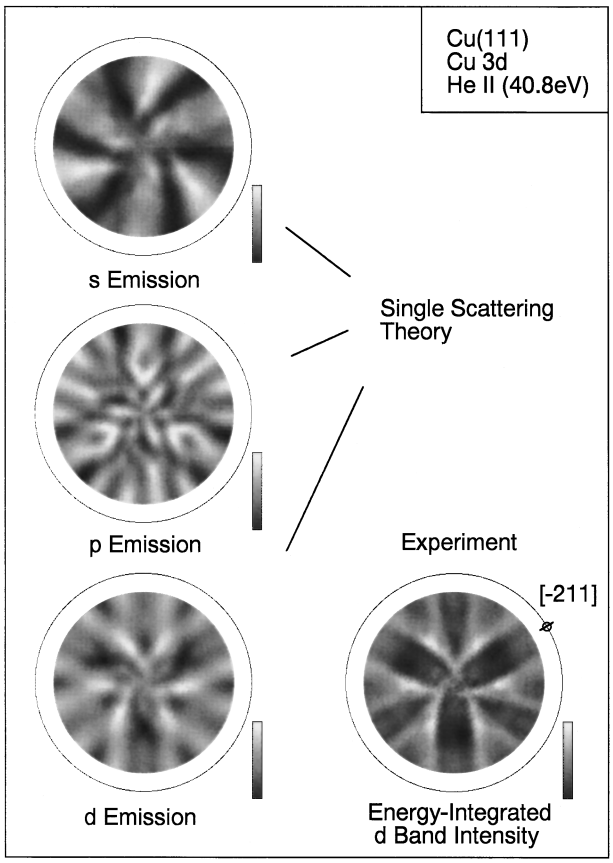

FIG. 5. Same as Fig. 4, but for excitation with He II radiation at 40.8 eV.

and SSC calculations for two faces of copper, Cu(111) and Cu(001), and for two different photon energies, He I (21.2 eV) and He II (40.8 eV) radiation. The experimental data are raw, except for the normalization procedure described in Sec. III, and no symmetry averaging has been performed. Calculations have been carried out for excitation from three different initial angular momentum states: *s*, *p*, and *d* emission. In each case the contributions of photoemitters from each of four layers at and below the surface have been summed.

The overall impression one obtains from Figs. 4 to 7 is quite striking: For each case the experimental pattern is by far best reproduced by the *d* emission calculation, and the agreement is in all cases remarkably good and almost quantitative. This statement is not only true for the appearance and symmetry of the patterns, but also for the absolute magnitude of the effect. As an illustration, Fig. 8 shows an azimuthal section through the data of Fig. 4, taken at a polar angle of 66° off normal. For this case, the maximum anisotropies, measured as $(I-I_{\min})/I_{\max}$, are 0.43 for the experiment and 0.36 for the calculation. While this is not fully quantitative, these numbers are nevertheless rather close if one remembers that emission anisotropies in higher-energy photoelectron diffraction are typically overestimated in single-scattering theory by a factor of 1.5 to 2.0 (Ref. 11). Here we have a case where the calculated anisotropies are slightly weaker than the measured ones. We conclude that such energy-integrated UV-excited photoelectron intensities are dominated by UV photoelectron diffraction (UPD) effects.

The degree of agreement we find between the experimental emission patterns and the *d* emission calculations is remarkable for two reasons: (i) Even though we consider emission from band states, which are delocalized enough to produce strong dispersion effects (Fig. 3), the 3*d* band of copper produces upon energy integration an intensity pattern that is well described by a model involving emission from individual localized *d* orbitals, and (ii) multiple scattering effects are expected to be strong at such low electron energies, but a single-scattering theory predicts the emission pattern rather well.

The second point is, in our view, the less fundamental one and can be intuitively understood. Fritzsche has recently discussed the effects of finite energy resolution on photoelectron diffraction spectra.[24] He showed that long scattering paths are systematically suppressed if the energy spread of the measured electrons is non-negligible with respect to their mean kinetic energy. Electrons at the lower and higher ends of the energy window have sufficiently different wavelengths

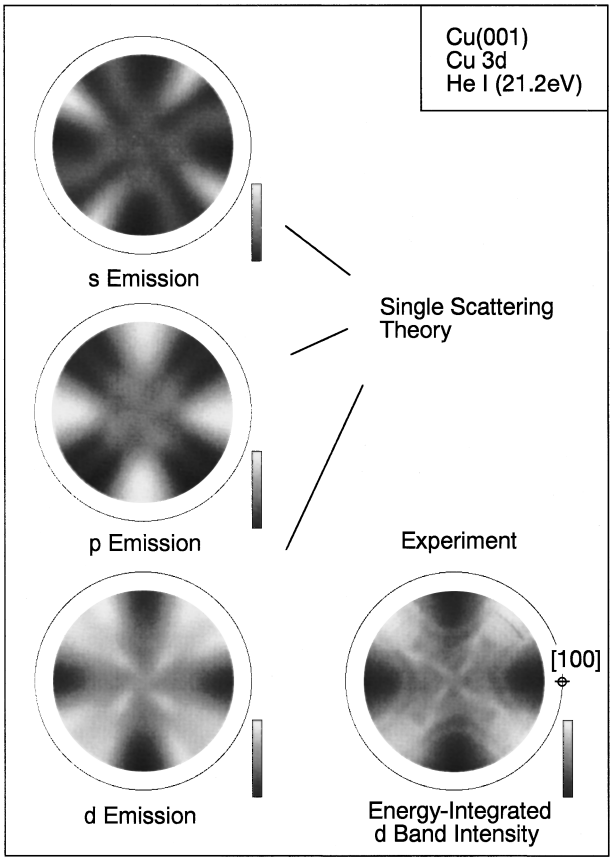

FIG. 6. Same as Fig. 4, but for Cu 3*d* electrons emitted from Cu(001) after excitation with He I radiation.

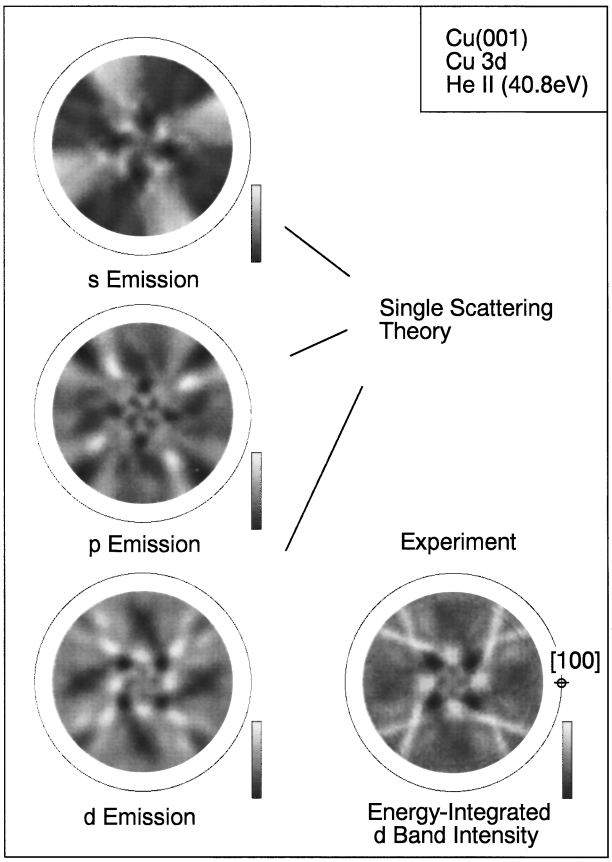

FIG. 7. Same as Fig. 4, but for Cu 3*d* electrons emitted from Cu(001) after excitation with He II radiation.

to run gradually out of phase. In our case we have a situation where the mean kinetic energy inside the solid is about 26 eV (He I) and 45.6 eV (He II), while the window width is 3.6 eV. Considering the associated spread in wave lengths, it takes path lengths of about 17 Å (He I) and 22 Å (He II) in order to have the lower and higher end electrons completely out of phase, and coherence is expected to be damped earlier than that. In our SSC calculations we have used cluster sizes of the order of 15 Å in diameter and 6 Å in depth, which are dimensions where such effects clearly begin to be important. Therefore, any improvement of these calculations in terms of including multiple scattering must at the same time include the energy spread of the electrons.

We now discuss the observed *duality* between the dispersion shown in these spectra, indicating states that extend over more than a single atomic site, and the intensity pattern which indicates emission from localized sources. A localization due to the emission process has been inferred from x-ray excited photoelectron diffraction data considering integrated valence band emission from Al(001) (Refs. 25 and 26). In this case, the pattern along an azimuthal scan, measured at a polar angle of $\theta=45°$, was found to be essentially identical to that of a near-lying core level (Al 2*s*), both in shape and in absolute anisotropies. Considering the nearly free electron nature of the *sp*-like valence band of aluminium, this apparent localization must be due to the photoemission process itself and/or due to the way we measure it. An obvious localization arises here because the final-state wave vectors are about ten reciprocal basis vectors long, which leads to an averaging over a large part of the Brillouin zone due to a combination of finite angular resolution, short electron escape depth, and phonon-assisted indirect transitions.[27] In order to see this, we consider the idealized case of photoemission from Bloch states given as a linear combination of Wannier functions:

$$\psi(\mathbf{k},\mathbf{r})=\frac{1}{\sqrt{N}}\sum_j e^{i\mathbf{k}\mathbf{R}_j}w(\mathbf{r}-\mathbf{R}_j). \tag{2}$$

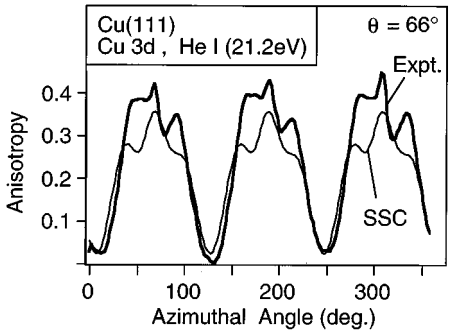

FIG. 8. Azimuthal section through the experimental data set of Fig. 4, taken at a polar angle of 66° (dark line) in order to permit a quantitative comparison of the measured intensity anisotropies, given as $[I(\phi)-I_{\min}]/I_{\max}$, with those obtained with a single-scattering calculation using localized *d*-wave emitters (thin line).

Here, N is the number of atoms in the crystal volume over which the summation is carried out, and $w(\mathbf{r}\text{-}\mathbf{R}_j)$ represents the Wannier function centered at the atomic site $\mathbf{R}_j$. The photoemission matrix element for emission into a free-electron final state of $e^{i\mathbf{k}_f r}$, with $\mathbf{k}_f$ being the photoelectron wave vector, can then be expressed as[28]

$$M_{if} \propto \int_{BZ} d^3k \left\langle \sum_j e^{i\mathbf{k}\mathbf{R}_j} w(\mathbf{r}-\mathbf{R}_j) \middle| \mathbf{p}\cdot\mathbf{A} \middle| e^{i\mathbf{k}_f\mathbf{r}} \right\rangle \delta(E_f - E_j - h\nu). \tag{3}$$

The integration over the Brillouin zone reflects the above-mentioned zone averaging effects which lead to a coherent superposition of emission processes from all initial state wave vectors $\mathbf{k}$. Carrying out the integration yields

$$\sum_j \int d^3k e^{i\mathbf{k}\mathbf{R}_j} = \sum_j \delta(\mathbf{R}_j) \tag{4}$$

and the matrix element becomes

$$M_{if} \propto \langle w(\mathbf{r}) | \mathbf{p}\cdot\mathbf{A} | e^{i\mathbf{k}_f\mathbf{r}} \rangle \delta(E_f - E_i - h\nu). \tag{5}$$

Clearly, the initial state has collapsed into a single Wannier function centered at one atomic site even if free-electron-like states are involved. As a consequence, coherent emission from several centers is not observed in this x-ray limit.

Aside from this localization due to zone averaging, more fundamental mechanisms for hole state localization in photoemission have been discussed. Specifically, exchange and correlation effects that give rise to the exchange-correlation hole in the free electron gas are also inferred to induce valence hole localization upon photoemission.[29,30] These ideas are supported by the observation of essentially the same intrinsic plasmon creation rates in core and valence electron emission, indicating a similar perturbation of the electron gas in both cases.[31]

The present data set corroborates the existence of localization phenomena that go beyond that of zone averaging: The observation of strong dispersion effects in the individual spectra gives clear proof that a small volume in $\mathbf{k}$ space is sampled at each angle. The energy integration gives a smearing of the magnitude of $\mathbf{k}$ of the order of 0.2 Å^{-1}, which is less than 10% of typical Brillouin zone dimensions, and by no means enough to explain the observed local emission pattern by zone averaging effects.

As an intermediate case of incomplete zone averaging, Herman *et al.*[32] measured, at room temperature, energy-integrated x-ray excited valence electron spectra of $W(110)$ as a function of azimuthal angle. Here, angular variations of the spectra are seen, while the resulting diffraction curves are rather similar to those of $W\ 4f$ with some significant deviations. From a comparison to fully zone averaged data measured at a temperature of 803 K, they concluded that these deviations should be partly due to different angular momentum final states (p and f for $W\ 5d$, d and g for $W\ 4f$) and partly due to remnant direct transition selection rules. In view of our current results these latter effects are not expected to influence the energy-integrated intensities. Indeed, in earlier work on tungsten by White *et al.*,[27] it was observed that direct-transition intensity must be lost at very nearly the same rate as nondirect-transition intensity is gained with increasing temperature, thus implying an empirical "sum rule."

In this context, we should mention that Thomann and Fauster[33] have integrated direct transition intensities, obtained within a parametrized band structure of Cu and weighted by transition matrix elements, for energies covering the $3d$ bandwidth. This procedure was performed for all $\mathbf{k}$-directions pointing outside the surface. The obtained angular distributions show some similarities with the measured distributions of Figs. 4–7, but there is significantly less overall agreement as compared to the present study. Therefore, even though this parametrized band structure describes the dispersion well, the underlying wave functions and/or the free-electron final state wave functions used for calculating the matrix elements are insufficient to describe the observed angular dependence of the integrated d band emission quantitatively. However, a very significant result appears from their study. They find that the angular distribution is dominated by the coupling of the plane waves inside the crystal to those in the vacuum rather than by the transition matrix elements.

Our observation suggests that cluster calculations of final-state scattering effects involving emission from localized orbitals may be an efficient way to calculate angular intensity variations of direct transitions. In order to see this we refer again to Fig. 1 where the dispersing transition from the sp band is shown. Contrary to the $3d$ band we have to consider a single band only in this case. The energy integration will here pick up directly the intensity modulations for transitions from this band. The complication is that the band moves across the Fermi level when $\mathbf{k}$ crosses the Fermi surface, and we can thus measure these effects only inside the Fermi surface. However, the experimental verification of whether the correspondence of energy-integrated angular distributions and emission patterns from localized sources holds also for cases with partially filled bands, in this case for selected contiguous regions in $\mathbf{k}$ space, remains to be done. The theoretical analysis may here be complicated by crystal field effects that cause a nonuniform occupancy of magnetic sublevels in the open shell. Theoretical analyses along these lines are underway.

VI. STRUCTURAL SENSITIVITY

The description of energy-integrated valence emission spectra in terms of final-state scattering opens up the possibility of obtaining structural information from such data, using an analysis scheme which is strongly related to that of x-ray photoelectron diffraction (XPD). Cluster models need to be conceived representing the surface geometry under study, and final-state scattering calculations are then carried out within the single-scattering cluster approximation described in Sec. IV. The atomic geometry of the cluster is varied in order to optimize the agreement with the experimental angular distributions.

There are some qualitative differences between the scattering of high-energy electrons encountered typically in XPD and the low-energy situation which is present here. At kinetic energies of ca. 300 eV and more, electrons are strongly scattered along the forward direction, giving rise to so-called

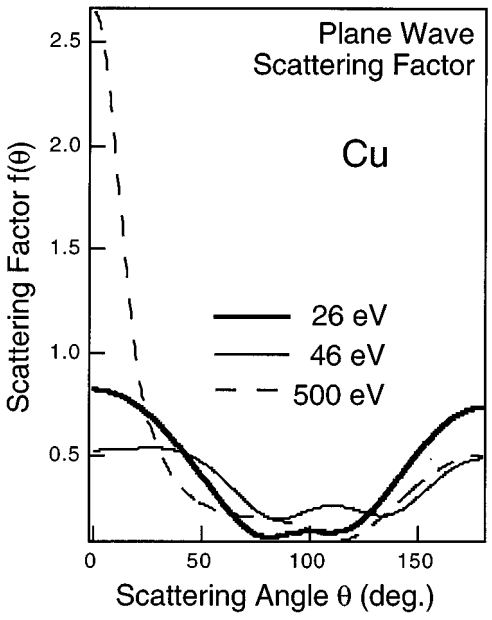

FIG. 9. Scattering factors for describing the scattering of a plane wave off a single Cu atom at three different electron energies. These curves have been calculated using partial wave phase shifts obtained from a Cu muffin-tin potential.[23]

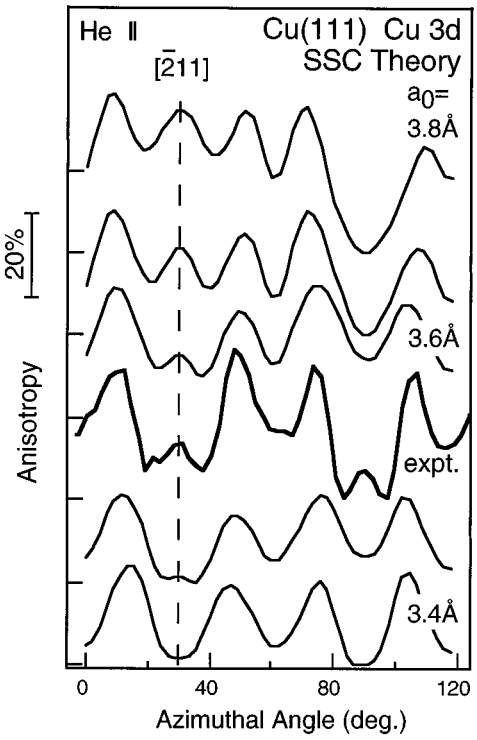

FIG. 10. Azimuthal section through the experimental data set of Fig. 5 [Cu(111), He II excitation], taken at a polar angle of 66° (dark line). In order to study the sensitivity of such data to bond lengths within the surface region, this curve is compared to several calculated curves (thin lines) obtained within the SSC model (*d* emission) and assuming various fictitious values for the lattice constant a_0 of Cu, ranging from 3.4 Å (bottom curve) to 3.8 Å (top curve).

forward-focusing maxima along interatomic bond directions. The main information obtained by XPD is thus purely geometric bond orientation, while bond length information is only contained in much weaker first- and higher-order interference fringes. Low-energy photoelectrons such as those produced upon UV excitation scatter much more isotropically (Fig. 9) and produce thus far stronger interference features. It is now of interest to know the sensitivity of these interference fringes to structural parameters, specifically the bond length.

First we present in Fig. 10 the results of SSC calculations for *d* emission from Cu(111), excited by He II radiation, for fictitious variations of the Cu lattice constant a_0. Over the range of a_0=3.4 Å to 3.8 Å we observe significant differences between each of these azimuthal curves taken at θ=66°, with increments in a_0 being 0.1 Å and thus less than 3%. We find slight angular shifts, changes in relative intensities, and for this polar angle the gradual appearance of an additional interference maximum along the [211] azimuth (ϕ=30°) with increasing lattice constant. The sensitivity to structure is thus similar to that of XPD when used for adsorbate emission,[34] and, in fact, superior to XPD when used for substrate emission where zero-order forward scattering dominates the emission pattern and bond length information is very limited.[12] In the same figure we also give an azimuthal section through the experimental data set of Fig. 5, at the same polar angle of 66°, in order to permit a quantitative comparison to the various calculated curves. As in Fig. 8 we find a rather good agreement in peak positions and overall anisotropies, especially for the calculation with the true lattice constant of 3.6 Å. Moreover, the relative intensity of the extra peak in the [211] azimuth is best reproduced for this value. Nevertheless, one also notices some deficits in the calculations which generally produce broader peaks than those experimentally observed and which fail to predict the small peak at ϕ=90°. It should be interesting to see whether residual multiple scattering effects can account for these deficits in our SSC calculations.

A further result from our analysis of structural effects on such angular patterns is that we find these curves to converge extremely rapidly with the number of emitting layers. The surface layer by itself reproduces the essential gross features of the angular distribution, which sharpen somewhat as further layers are added. After three layers there is essentially no more change. All these calculations were carried out assuming an inelastic mean free path of 5 Å, which in our SSC model corresponds to an exponential decay length of wave amplitude of 10 Å (Ref. 35). Further reducing this value does not help to produce sharper features.

VII. CONCLUSIONS

We have found a remarkable duality in the way UV-excited Cu 3*d* photoelectron spectra from clean Cu surfaces exhibit both itinerant and localized character at the same time. Energy-resolved spectra show pronounced dispersion effects thus reflecting the band nature of these electrons, while upon energy integration the resulting angular intensity distributions indicate emission from sources localized on individual lattice sites. These experiments provide further hints for the localization of a valence hole upon photoemission.[30] The emission pattern is dominated by final-state scattering, i.e., by UV photoelectron diffraction (UPD) effects, which

we can well describe within a single-scattering cluster (SSC) model. The observed structural sensitivity of such UPD patterns is relevant for two aspects: It permits the analysis of surface structure using a UV source, thus combining detailed structural and electronic information in one experiment. Moreover, it means that measured intensities of direct transition peaks will depend rather strongly on the geometrical arrangement of the surface atoms.

ACKNOWLEDGMENTS

We thank A. Stuck and D. Naumovic for their help in performing these experiments, and T. Fauster, V. Fritzsche, and S. Hüfner for invaluable discussions. Excellent technical support was given by O. Raetzo, F. Bourqui, E. Mooser, and H. Tschopp. This work was supported financially by the Swiss National Foundation.

[1] E. W. Plummer and W. Eberhardt, Adv. Chem. Phys. **49**, 533 (1982).
[2] S. Hüfner, *Photoelectron Spectroscopy* (Springer-Verlag, Berlin, 1995); R. Courths and S. Hüfner, Phys. Rep. **112**, 53 (1984).
[3] S. D. Kevan, Phys. Scr. **T31**, 32 (1990).
[4] N. V. Smith, Comments Cond. Mat. Phys. **15**, 263 (1992).
[5] I. Adawi, Phys. Rev. A **134**, 788 (1964).
[6] G. D. Mahan, Phys. Rev. B **2**, 4334 (1970).
[7] A. Liebsch, Phys. Rev. Lett. **32**, 1203 (1974).
[8] J. B. Pendry, Surf. Sci. **57**, 679 (1976).
[9] N. V. Smith, M. M. Traum, Phys. Rev. B **11**, 2087 (1975).
[10] A. Liebsch, Solid State Commun. **19**, 1193 (1976).
[11] C. S. Fadley, in *Synchrotron Radiation Research: Advances in Surface and Interface Science*, edited by R. Z. Bachrach (Plenum, New York, 1992), Chap. 11.
[12] J. Osterwalder, T. Greber, A. Stuck, L. Schlapbach, Phys. Rev. B **44**, 13764 (1991).
[13] A. Santoni, L. J. Terminello, F. J. Himpsel, and T. Takahashi, Appl. Phys. A **42**, 299 (1991).
[14] J. Osterwalder, A. Stuck, T. Greber, P. Aebi, L. Schlapbach, and S. Hüfner, *Proceedings of the 10th International Conference on VUV Radiation Physics*, edited by F. J. Wuilleumier, Y. Petroff, and I. Nenner (World Scientific, Singapore, 1993), p. 475.
[15] P. Aebi, J. Osterwalder, R. Fasel, D. Naumovic, L. Schlapbach, Surf. Sci. **307–309**, 917 (1994).
[16] P. Aebi, J. Osterwalder, P. Schwaller, L. Schlapbach, M. Shimoda, T. Mochiku, and K. Kadowaki, Phys. Rev. Lett. **72**, 2757 (1994).
[17] P. Aebi, T. J. Kreutz, J. Osterwalder, R. Fasel, P. Schwaller, and L. Schlapbach, Phys. Rev. Lett. **76**, 1150 (1996).
[18] D. Naumovic, A. Stuck, T. Greber, J. Osterwalder, and L. Schlapbach, Phys. Rev. B **47**, 7462 (1993).
[19] M. Sagurton, E. L. Bullock, and C. S. Fadley, Surf. Sci. **182**, 287 (1987).
[20] J. J. Rehr and R. C. Albers, Phys. Rev. B **41**, 8139 (1990).
[21] D. J. Friedman, C. S. Fadley, J. Electron Spectrosc. Relat. Phenom. **51**, 689 (1990).
[22] S. M. Goldberg, C. S. Fadley, and S. Kono, J. Electron Spectrosc. Relat. Phenom. **21**, 285 (1981).
[23] J. B. Pendry, *Low Energy Electron Diffraction* (Academic, London, 1974).
[24] V. Fritzsche, Surf. Sci. **265**, 187 (1992).
[25] J. Osterwalder, T. Greber, S. Hüfner, and L. Schlapbach, Phys. Rev. Lett. **64**, 2683 (1990).
[26] D. D. Sarma, W. Speier, and J. F. van Acker, Phys. Rev. Lett. **66**, 2834 (1991), Comment; J. Osterwalder, T. Greber, L. Schlapbach, S. Hüfner, *ibid*., Reply.
[27] R. C. White, C. S. Fadley, M. Sagurton, Z. Hussain, Phys. Rev. B **34**, 5226 (1986).
[28] P. J. Feibelman and D. E. Eastman, Phys. Rev. B **10**, 4932 (1974).
[29] D. R. Penn, Phys. Rev. Lett. **40**, 568 (1978).
[30] C. O. Almbladh and L. Hedin, in *Handbook on Synchrotron Radiation*, edited by E. E. Koch (North-Holland, Amsterdam, 1983), Vol. 1B, p. 683.
[31] H. Höchst, P. Steiner, S. Hüfner, Z. Phys. B **30**, 145 (1978).
[32] G. S. Herman, T. T. Tran, K. Higashiyama, and C. S. Fadley, Phys. Rev. Lett. **68**, 1204 (1992).
[33] U. Thomann and T. Fauster (unpublished).
[34] R. Saiki, A. P. Kaduwela, Y. J. Kim, D. J. Friedman, J. Osterwalder, S. Thevuthasan, and C. S. Fadley, Surf. Sci. **279**, 305 (1992).
[35] J. Osterwalder, A. Stuck, D. J. Friedman, A. P. Kaduwela, C. S. Fadley, J. Mustre de Leon, and J. J. Rehr, Phys. Scr. **41**, 990 (1990).